Multi-objective optimisation and guidelines for the design of dispatchable hybrid solar power plants with thermochemical energy storage.

R.Bravo[a,1], C.Ortiz[b], R.Chacartegui[c], D.Friedrich[a,*]

[a]*School of Engineering, Institute for Energy Systems, The University of Edinburgh, UK*
[b]*Departamento de Ingeniería, Universidad Loyola Andalucía, Av. de las Universidades s/n, Dos Hermanas, 41704, Sevilla, Spain*
[c]*Departamento de Ingeniería Energética, Universidad de Sevilla, Camino de los Descubrimientos s/n, 41092, Sevilla, Spain*

Abstract

The drive to net zero energy requires high renewable penetration but most renewables are either affordable or dispatchable but not both. Thermochemical energy storage integrated into concentrating solar power plants can enhance dispatchability and solar-to-electricity efficiency. Combining these technologies with lower cost photovoltaic plants exploits synergies related to dispatchability and costs. However, this combination leads to complex interactions between the different power plant components and requires sophisticated design guidelines to simultaneously achieve low costs and high dispatchability. Here, we develop multi-objective optimisations and guidelines for the design of hybrid solar power plants with a calcium-looping thermochemical energy storage system. The applied tools presented focus on the optimisation of the design and operation of hybrid power plants plants with respect to competing technical and financial performance metrics. First, the design optimisation stage evaluates ten design variables and three objectives. Then, the operational optimisation stage, which is nested inside the design stage, finds the best one-year hourly operational strategy for each configuration considered in the first stage. We evaluated three case studies with different solar resource: Seville (Spain), Tonopah (United States), and the Atacama Desert (Chile). The best dispatchable hybrid solar power plant with an Levelised cost of electricity of 123 USD·MWh^{-1} and a capacity factor of 73% is reached for the Atacama Desert, which has the best solar resource. The optimisation results are used to develop guidelines for the optimal design of dispatchable hybrid solar power plants with CaL based on the given solar resource and required dispatchability. These guidelines provide an initial design for affordable and dispatchable hybrid solar power plants and can enable their widespread deployment.

Keywords: Two-stage optimisation, Multi-objective optimisation, Concentrating solar power, Photovoltaic systems, Calcium-looping, Thermochemical Energy storage

Context & scale

The greenhouse gas emissions of the electricity sector must be reduced to prevent a substantial rise in global temperature. Renewable electricity generation technologies are crucial for this emissions reduction and to promote sustainable development. It is essential to develop affordable and dispatchable renewable power plants to achieve the widespread deployment of clean energy technologies. Current research on thermochemical energy storage systems has shown that the combination of calcium-looping in large scale concentrating solar power plants enhances the dispatchability and the solar-to-electricity efficiency of solar thermal energy technologies. The hybridisation with solar photovoltaic plants improves the affordability of solar power plants while maintaining the dispatchability. However, the variability of the solar resource and the integration of energy storage requires the use of sophisticated techniques for the optimal design of hybrid power plants. This article presents a multi-objective optimisation framework focused on finding an optimal design of a hybrid power plant while determining the best strategy for its operation, handling the trade-offs between conflicting technical and financial performance metrics. The guidelines presented in this research are expected to enable the economic design of dispatchable hybrid solar power plants.

1. Introduction

The large and fast deployment of renewable energy technologies is crucial to reduce greenhouse gas emissions so that we can reach a long-term balance between sources and sinks and avoid a rise in global temperature higher than 2 °C [1]. Renewable generation technologies are fundamental to decarbonise the power sector but need to be

*Corresponding author
Email address: d.friedrich@ed.ac.uk (D.Friedrich)

[1]The author is supported by a PhD student scholarship from BECAS CHILE, CONICYT. Ruben Bravo is currently affiliated with the Department of Electrical & Electronic Engineering, The University of Manchester, Manchester M13 9PL, UK.

integrated with energy storage to provide dispatchable energy [2, 3]. In this context, photovoltaic (PV) is one of the best alternatives to provide affordable but intermittent power [4]. PV plants can be made more dispatchable if they are combined with electrical energy storage (EES) systems (e.g. batteries). However, batteries are expensive (around 300 - 550 USD·kWh^{-1}) and the scarcity of the raw materials (e.g. lithium) compromises their viability for large scale applications [5]. On the other hand, thermal energy storage (TES) can be up to two orders of magnitude cheaper than electricity storage [6]. A potential alternative to increase the dispatchability and affordability of solar power plants is the hybridisation PV plants with concentrating solar power plants (CSP) integrated with [7, 8]. This manuscript combines the hybridisation and advanced TES systems with multi-objective design optimisation.

CSP plants integrated with TES have the potential to provide dispatchable power [9, 10]. TES systems can be divided into three concepts. The first concept, currently developed in commercial CSP plants, is sensible thermal energy storage [11]. In this context, molten-salt technologies are the most deployed technology in CSP plants [12]. This system uses differences in the temperature of a substance to store energy. The second is latent heat, by using the enthalpy of phase change of a suitable material [13, 14]. Finally, thermochemical energy storage (TCES) which is the primary technology evaluated in this research uses the enthalpy of a reversible chemical reaction. TCES is a promising technology with the potential for high energy storage densities and no storage losses (beside the initial loss of the sensible heat) [15].

TES systems are typically based on the two-tank molten salt technology. This technology has several disadvantages that decrease the performance of CSP and provide opportunities to develop better alternatives. First, the efficiency is constrained by the technical limitations of the working temperature of the process (560°C), that is required to avoid the degradation of the material [16]. Second, a minimum temperature of 200°C is needed to prevent solidification of the salts, which requires a substantial amount of energy when the plant is not operational [17]. Finally, the high corrosiveness of the salt requires the use of suitable materials for storage and transport that increase the investment costs of the system [18].

TCES operates with a reversible chemical reaction, absorbing the heat harvested by the solar field of the CSP plant to perform an endothermic reaction and to store energy [15]. When energy is needed, the reverse exothermic reaction is used to release the stored energy. Different TCES systems integrated with CSP plants have been under study and development [19]. Whilst some TCES systems work at high temperature, hence, high efficiency when integrated into CSP plants (e.g. calcite calcination/carbonation) [20], other processes work at lower temperature and are more suitable for industrial waste heat applications (e.g. magnesium oxide, 350 to 400 °C) [21]. A reversible process that has received significant attention for the implementation into CSP plants is the calcination/carbonation of calcite, with a working temperature in the range of 700 - 1000 °C [22].

This process, known as calcium-looping (CaL), involves calcium carbonate ($CaCO_3$), calcium oxide (CaO) and carbon dioxide (CO_2). The cyclic calcination-carbonation of calcium carbonate and calcium oxide is given by equation 1.

$$CaCO_{3(s)} \rightleftarrows CaO_{(s)} + CO_{2(g)} \qquad \Delta\hat{H}_r^{\circ} = 178\ kJ \cdot mol^{-1} \tag{1}$$

The CaL process has important advantages that make it an attractive and promising technology as a TCES system [23, 24]. For instance, the abundance and low price of the precursor materials (i.e. limestone or dolomite), the properties of the products (non-corrosive, non-toxic) [20, 25], and its theoretical high energy density (4.4 GJ·m^{-3}) [26]. Due to its great potential, and its early development stage, different studies have focused on the analysis of CaL as a TCES process integrated into CSP plants [23].

Current studies focus on the development of improved materials and process conditions to decrease its deactivation due to the multi-cyclic operation requirements [27, 28]. Moreover, the high-temperature energy released in the CaL process allows the integration of high-efficiency power cycles [29]. Therefore, the CaL process integrated into CSP plants has the potential to supply dispatchable power [22]. More details on the CaL process and its integration in CSP can be found in Chacartegui, Alovisio, Ortiz, Valverde, Verda, and Becerra [22], and Ortiz, Chacartegui, Valverde, Alovisio, and Becerra [29].

Recent optimal operational studies of hybrid power plants with energy storage have been focused on the analysis of single objectives [30], or the evaluation of a limited temporal resolution representing the analysis of a whole year [31, 32]. In this context, Ortiz, Romano, Valverde, Binotti, and Chacartegui [15] conclude that hourly simulations considering variable solar irradiation need to be investigated to improve the analysis in the integration and design of CSP plants with CaL. The one-year hourly operational optimisation allows analysing a large time frame, which is necessary to evaluate the long-term and seasonal behaviour of the system under variable solar resource [33].

In addition, the concept of optimal design of hybrid CSP-PV plants exploits technical and economic synergies of both technologies, has the potential to reduce operational and capital costs, and to increase the capacity factors of solar technologies [34, 35]. For instance, Green, Diep, Dunn, and Dent [36] studied the integration of a PV plant in the Crescent Dunes CSP project, concluding that the hybridisation can raise the capacity factor to over 80%. A similar study was carried out in Northern Chile, showing that a hybrid CSP-PV provides a levelised cost of electricity (LCOE) of 121 USD·MWh^{-1}, compared with 128 USD·MWh^{-1} for standalone CSP systems [35].

Bravo, Ortiz, Chacartegui, and Friedrich [37] developed a multi-objective linear scalarisation method to find the best operational strategy considering hourly time steps and one-year operation. This study evaluated different designs to analyse the synergies of technology integration, concluding that a design optimisation routine needs to be investigated and implemented to improve the affordability and dispatchability of solar power plants considering variable solar resource. However, the existing studies do not exploit the synergies of large scale hybrid solar power plant systems integrated with thermochemical energy storage by optimising financial and technical performance in both the design and the operational optimisation stages.

To design a dispatchable and also affordable energy system, a multi-objective design optimisation stage is necessary to select the right size of the main components. On the one hand, if one component of the CaL is undersized, there will be a bottleneck in the operation, that results in a reduction in the efficiency of the whole process. On the other hand, the oversizing of a component will result in an unnecessary high investment cost, increasing the LCOE.

The design of hybrid solar power plants with TCES requires sophisticated design tools due to the complex interactions between different elements of the plant. These tools need to balance the trade-offs between financial and technical performance metrics in order to design affordable and dispatchable solar power plants. The optimisation of a solar power plant has been studied by Kalogirou [38], using artificial neural networks to analyse the simulations of its operation and genetic algorithms to optimise its design. A multi-objective approach for the optimal size of a hybrid CSP-PV power plant integrated with thermal energy storage has been implemented by Starke, Cardemil, Escobar, and Colle [35]. In this study, the design optimisation focusing on the analysis of the trade-off between costs and capacity factor is developed by a genetic algorithm coupled with a surrogate model for each objective function. To build the surrogate model, an annual simulation of the operation estimates the thermal and economic performance of each power plant by a transient model. In a previous study [39], an optimisation framework to optimise the design of a CSP with thermal energy storage (using molten salts), and the operation by linear programming was developed, concluding that the analysis of the trade-off between technical and economic performance is key to design an affordable and dispatchable power plant. Moreover, the direct link between the objectives of the design and operational optimisation routines is crucial to exploit the synergies of different technologies.

Applied studies of TCES integrated into CSP plants have been focused on Europe, e.g. Seville, Spain [40]. Nevertheless, according to the IEA [41], locations close to the Tropics (Capricorn and Cancer), with clear skies and high solar irradiation have the best condition for the development of CSP technologies. However, each location requires a bespoke design due to the complex interactions between the different parts of the system and the differences in solar resource profile. Hence, to analyse projects under development, and potential locations for further deployment of solar plants with TCES, the following locations which cover a range of different profiles will be evaluated: Seville, Spain; Tonopah, Nevada, United States; and the Atacama Desert, Chile. While Northern Chile has one of the highest solar irradiations in the world, Nevada and Southern Spain are among the sunniest region in the United States and Europe respectively. Moreover, power tower CSP projects in operation or under construction can be found in these areas, for instance, Gemasolar Thermosolar Plant (Seville), Crescent Dunes Solar Energy Project (Tonopah), Atacama-1 (Chile) [42].

Hence, the main focus of the present research is to optimise the design of a hybrid solar power plant integrated with CaL as TCES with the aim of exploiting synergies of technology integration. In order to evaluate the long-term and seasonal behaviour of the system under variable solar resource, the two-stage, multi-objective optimisation framework developed in this study optimises the sizing of the main components (design) and the strategy to operate under variable solar resource (operation). The multi-objective design and operational optimisation considers technical and economic performance to design a dispatchable and cost-competitive power plant, exploiting synergies of CSP with CaL (dispatchability) and PV (affordability). Besides, the optimisation results are used to develop guidelines for the optimal design of dispatchable hybrid solar power plants with CaL based on the given solar resource and required dispatchability. The proposed framework provides a systematic methodology and guidelines for the design of dispatchable power plants for any location with a good solar resource, taking the yearly operation into account and goes beyond a manual design process.

2. Methodology

In order to design an affordable and dispatchable solar power plant, the trade-off between financial and technical performances has to be examined. While an oversized CSP plant can give us full dispatchability at a high LCOE, a PV plant will be more affordable, but not dispatchable. These conflicting objectives are handled by a multi-objective optimisation method which produces a range of non-dominated or Pareto optimal solutions. The design optimisation stage is based on the two-stage optimisation framework developed in Bravo and Friedrich [39] and extended here to a hybrid CSP-PV-TCES plant. Figure 1 shows the methodology adapted for the present research.

This framework uses a genetic algorithm (GA) to optimise the design of the power plant under techno-economic objectives. There are ten variables to consider and three objectives to evaluate (which are non-convex; hence, many local minima can exist in the design space). The use of genetic algorithms allows us to handle non-convex objectives

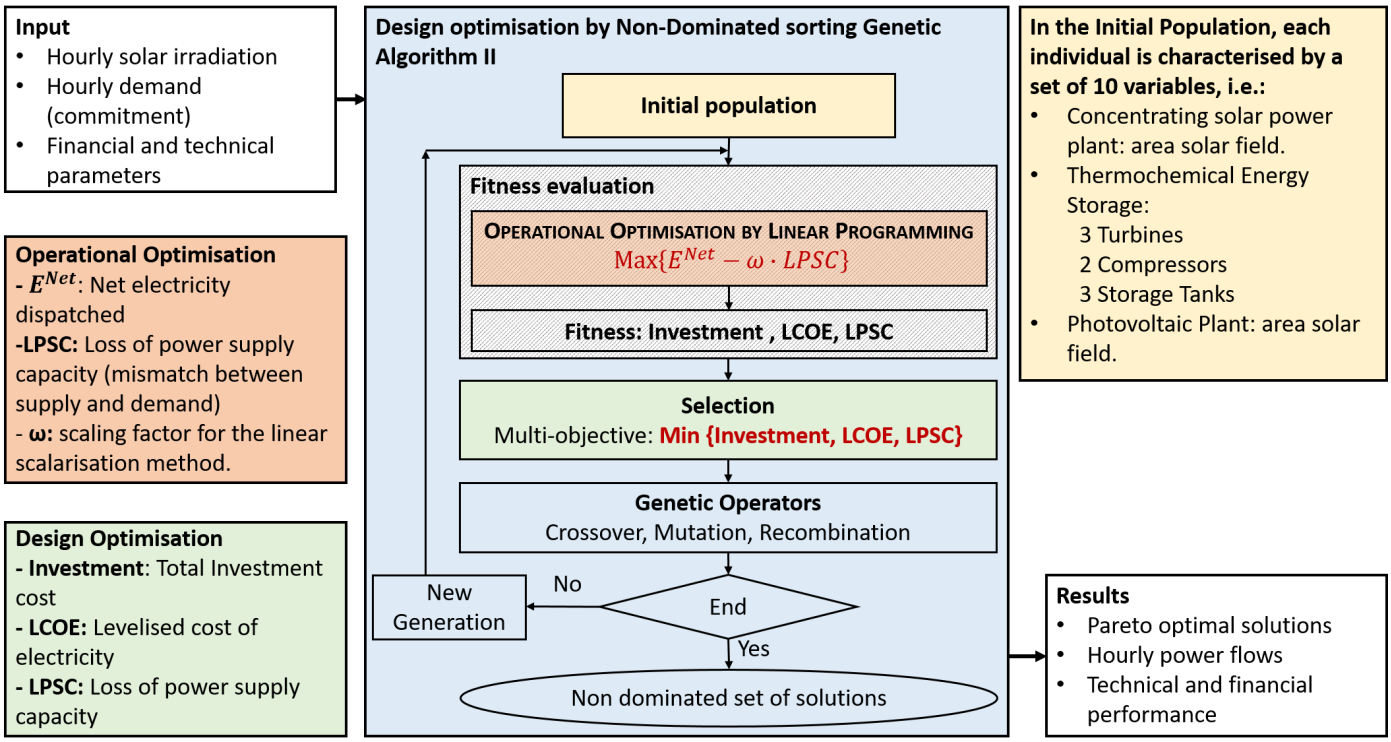

Figure 1: Schematic of the two-stage optimisation framework of the hybrid CSP-PV with TCES power plant

and several variables. The multi-objective design optimisation produces a range of Pareto optimal solutions, representing the trade-off between objectives.

As can be seen in Figure 1, the GA starts with an initial population, where each individual represents a power plant with given capacities. Then, each individual design in the population is optimised by using the operational optimisation by linear programming detailed below. Hence, the operation of each individual design of the genetic algorithm stage is optimised, considering one-year hourly solar irradiation. After the operational optimisation is performed, the investment cost, LCOE, and LPSC (Loss of Power Supply Capacity) are calculated and used by the GA to perform the fitness evaluation. After that, the genetic operators work to define the best offspring and then a new generation is produced. Finally, the stopping criteria used in our model is when the number of generations reaches a defined value. For the optimisation, we define 100 individuals for the initial population (100 combinations of independent design variables) and 100 generations as stopping criteria.

The operational optimisation is handled by our validated operational optimisation model presented previously [37]. Briefly, a multi-objective linear scalarisation routine for the operational optimisation is nested in the GA as a fitness function, linking the objectives of both stages. In Bravo, Ortiz, Chacartegui, and Friedrich [37], this multi-objective operational optimisation was used to find the best operational strategy of a hybrid CSP-PV plant with CaL by linear programming, considering one year of variable solar resource with hourly time-steps. The use of linear programming ensures a good approximation of the best operational strategy for one year of operation, considering variable solar resource, in a reasonable computational time. The operational optimisation routine simultaneously maximises the energy dispatched and minimises the mismatch between supply and demand.

Figure 2, adapted from [37], shows the mass and energy flow diagram of the proposed hybrid plant as well as the design and operational optimisation variables. In the first design stage of the optimisation routine, the variables are defined as capacities of the main components of the hybrid solar power plant with energy storage. These variables are shown in the red ovals in Figure 2. Meanwhile, in the second operational stage of the optimisation routine, the variables are associated with the mass/energy flows throughout the main processes of the plant, i.e. solar field, calciner, heat exchangers, superheated steam Rankine cycle, compressor and turbines, carbonator and storage tanks. These variables are illustrated with black circles in Figure 2.

Figure 2 illustrates the operation of the hybrid solar power plant with CaL. Concentrated solar irradiation from the heliostat field is used as a heat input at the solar receiver for the calcination of calcium carbonate ($CaCO_3$, solid) to calcium oxide (CaO, solid) and carbon dioxide (CO_2, gas). In this research, short residence times and complete calcination are considered when the reaction takes place at atmospheric pressure and a temperature around 900°C [27, 43]. CaO and CO_2 streams at high temperature

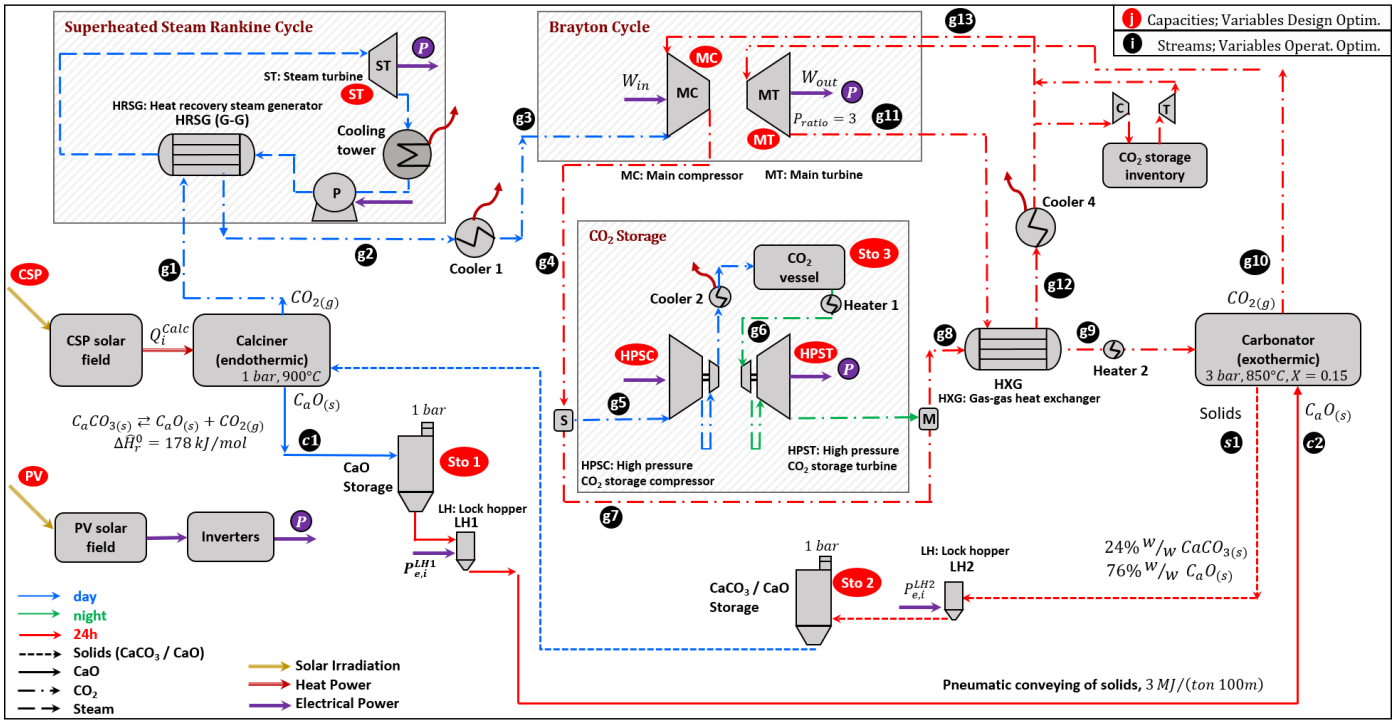

Figure 2: Mass and energy balances model of the hybrid solar power plant with CaL as TCES, adapted from [37]

(900 °C) leave the calciner to be stored in different tanks at ground level. Conveyors, equipped with lock hoppers to balance the pressure differences, are used to transport the calcium oxide from the calciner to an insulated tank at high temperature and atmospheric pressure. The CO_2 stream is stored in a high-pressure tank at atmospheric temperature by using compressors and heat exchangers. To increase the efficiency of the power plant, part of the heat released by the CO_2 before compression is used as a heat input in a small-size Rankine cycle. When energy is needed, the carbonator drives the exothermic reaction, which releases heat by mixing CaO and CO_2, generating $CaCO_3$. In this case, the carbonator works at 3 bar, and a CaO molar conversion of $X = 0.15$ is assumed [23]. To generate power, the heat released during the reaction is used to increase the temperature of the CO_2 stream (here well in excess), and then, this stream runs a gas turbine. After that, heat exchangers are used as a regenerative system to increase the efficiency of the process.

Finally, the photovoltaic power plant produces electricity during sunshine hours. Here we consider the use of monocrystalline silicon modules with nominal efficiency of 19%, and 60 kW_{ac} inverters [44]. While the PV power plant does not directly interact with the CaL storage system, the net electricity dispatched from the hybrid plant to the grid is the result of the power generation from the CSP with CaL system plus the generation from the PV plant minus all own consumption of the power plant.

During sunshine hours, PV is used to produce power directly whilst CSP produces electric power through the CaL integration, storing on the other hand a certain amount of thermochemical energy. When there is no solar radiation available to cover the demand, the production of electricity is carried out exclusively from the stored thermochemical energy. This operating procedure is similar to the one designed for the Cerro Dominador Solar Thermal Plant at Atacama Desert which uses a molten salt thermal energy storage system [45].

2.1. Variables: size of main components

The design of the power plant is given by the size of the following components, highlighted with the red ovals in Figure 2, which are defined as variables in the design optimisation routine:

- CSP plant with CaL TCES system:
  1. Heliostat solar-field aperture area: A^{CSP} (m^2)
  2. Steam turbine capacity: P^{ST} (MW)
  3. Main CO_2 compressor capacity: P^{MC} (MW)
  4. Main CO_2 turbine capacity: P^{MT} (MW)
  5. High-pressure CO_2 compressor capacity: P^{HPSC} (MW)
  6. High-pressure CO_2 turbine capacity: P^{HPST} (MW)
  7. CO_2 storage tank capacity: STO^{CO_2} (m^3)
  8. CaO storage tank capacity: STO^{CaO} (m^3)
  9. $CaCO_3$+CaO storage tank capacity: STO^{Solids} (m^3)
- PV plant
  10. Photovoltaic modules aperture area: A^{PV} (m^2)

As mentioned previously, each individual in the design optimisation, which is defined through these design variables, corresponds to a specific power plant with known capacities. As can be seen in Figure 1, the operational optimisation is nested inside the fitness evaluation of the design optimisation. Hence, the operation of each power plant design is optimised by linear programming. The focus of that stage is to maximise both, the energy dispatched and the dispatchability, which are usually conflicting objectives. Finally, three indicators (detailed in section 2.2) are considered as objectives of the design optimisation stage and used by the genetic operators.

2.2. Objectives: financial and technical performance

As stated previously, the design optimisation aims to select the optimal sizes of the components to design an affordable and dispatchable power plant. In this study, the total investment cost and the LCOE are employed to measure the affordability while the loss of power supply (LPS) is used to measure the dispatchability.

The total investment cost is estimated using the references summarised in Table 1. The data required to estimate the investment cost of a concentrated solar power plant, i.e. the heliostat field and the solar tower were obtained using the System Advisor Model (SAM) [42]. Here, the cost of the solar field (including the solar tower) was estimated as a function of the heliostats field. The investment cost of the solar tower was incremented by 10% to consider the installation and connections of the calciner located inside the receiver chamber. Besides, SAM was used to have an estimation of the total land area required for the whole project (CSP and PV). References and procedures to estimate the investment costs of the main components of the CaL system (i.e. calciner, steam power cycle, carbonator, heat exchangers, cooling towers, compressors, turbines and storage tanks) are summarised in Table 1. An average exchange rate of $r_x = 1.18$ (EUR to USD, 2018) was considered in this study to convert to Euros the estimated costs from some references [46].

Then, the LCOE is calculated by equation 2 [51],

$$\text{LCOE} = \frac{\sum_{t=0}^{T} \frac{C_t}{(1+r)^t}}{\sum_{t=1}^{T} \frac{E_t}{(1+r)^t}} \tag{2}$$

where C_t is the cost in period t (i.e. initial capital investment, annual operational and maintenance costs), and E_t is the energy dispatched in year t. In addition, values for the annual interest rate and a lifetime of $r = 7\%$ and $T = 25$ years, respectively, are used to be able to compare with other technologies and reports (e.g. IEA [52]).

According to equation 2, the LCOE is directly related to the investment, and more significant investment should result in a larger LCOE. Nevertheless, power plants with different designs but similar investments can dispatch different amounts of energy. Hence, a direct correlation between investment and LCOE is not always guaranteed.

Finally, to measure the ability to supply energy when it is needed (dispatchability), the loss of power supply (LPS) is used. Considering the subscript i as period (hours), the LPS measures the mismatch between supply (P_i^{net}) and commitment ($P_i^{\text{commitment}}$) in period i, according to:

$$\text{LPS}_i = \begin{cases} P_i^{\text{commitment}} - P_i^{net} & , P_i^{\text{commitment}} > P_i^{net}, \\ 0 & , \text{otherwise.} \end{cases} \tag{3}$$

To compare the results with the non-optimised hybrid solar power plants presented in Bravo, Ortiz, Chacartegui, and Friedrich [37], we define a permanent power commitment. Moreover, to avoid an oversize PV plant, and hence, a significant difference in the dispatch between day and night, the operational optimisation model was constrained by defining a maximum power dispatch five times the commitment.

$$P_i^{\text{commitment}} = 13.5\ MW,\ \forall i \tag{4}$$

$$P_i^{net} \leq 67.5\ MW,\ \forall i \tag{5}$$

Nevertheless, these capacities can be defined by the user according to the objectives pursued and the transmission constraints of the power plant.

The LPS is summed to the loss of power supply capacity (LPSC) which is used in the optimisation framework. To facilitate the final analysis, the LPSC value is reported as a percentage of the annual commitment which is given by the loss of power supply probability (LPSP, equation 7).

$$LPSC = \sum_{i=1}^{8760} LPS_i \tag{6}$$

$$LPSP = \frac{LPSC}{P_i^{Commitment} \cdot 8760} \tag{7}$$

A minimum constant power commitment of 13.5 MW has been considered for the plant. The power commitment is defined as the minimum power to be provided continuously by the plant throughout the year. The annual mismatch between supply and commitment (MWh), as a percentage with respect to the total annual commitment (MWh) is indicated by the Loss of Power Supply Probability (LPSP) concept, as shown in Equations 3, 6 and 7. Note that net power produced by the plant in sunshine conditions can be higher than the minimum power commitment, but it should not be less to ensure a specific dispatchability. The choice of a constant power commitment has been made for two reasons: i) for greater clarity when presenting the results and ii) to generalize the concept so that it is not dependent on a specific demand profile, since the variability of the electricity demand does not follow the same tendency in the selected locations. Thus, in Seville the demand increases in summer due to the extreme temperatures and high use of air conditioning, while in the Atacama Desert the demand is almost constant due

Table 1: References for estimating the investment costs of the main components of the power plant. Adapted from Bravo, Ortiz, Chacartegui, and Friedrich [37]

Component	Scaling parameter	Investment cost (IC) in MUSD	Ref.
CSP field & tower	Heliostats area (m^2)	See references for calc. procedure	[42]
PV plant	Photovoltaic area (m^2)	See references for calc. procedure	[42]
Total land area	CSP & PV (ha)	IC= $25 \cdot Area \cdot 10^{-3}$	[42]
Steam power cycle	Gross capacity (kW_e)	IC= $(290 + 1040) \cdot P_{max}^{\mathrm{ST}} \cdot 10^{-6}$	[42]
Calciner	Thermal Power (kW_{th})	IC= $(13140 \cdot Q_{calc}^{0.67} \cdot 10^{-6}) \cdot r_x$	[47]
Carbonator	Thermal Power (kW_{th})	IC= $(16591 \cdot Q_{carb}^{0.67} \cdot 10^{-6}) \cdot r_x$	[47]
Heat exchangers	Area (m^2) and P (bar)	IC= $(2546.9 \cdot A_{HE}^{0.67} \cdot P_{HE}^{0.28} \cdot 10^{-6}) \cdot r_x$	[47]
Cooling towers	Thermal Power (kW_{th})	IC= $(32.3 \cdot Q_{cool} \cdot 10^{-3}) \cdot r_x$	[47]
Compressors & turb.	-	See reference for calc. procedure	[48]
CO_2 storage tanks	-	See reference for calc. procedure	[49]
Solids storage tanks	-	See references for calc. procedure	[50, 49]

to the high energy intensity of the process associated with the copper mining industry. While the integration of the demand side is outside the scope of this manuscript, we are planning to combine the optimisation framework with energy system planning tools in the future.

2.3. Implementation

For the present research, a model written in Python was developed to optimise the design optimisation of the power plant with TCES. DEAP was employed inside the code to carry out the genetic algorithm routine [53]. Here, the fitness evaluation of each individual is performed by solving the operational optimisation stage using Pyomo [54] with Gurobi as solver [55]. In addition, real solar irradiation data is used as input, and it can be easily modified to evaluate any location. In summary, the hardware and software used to perform the optimisation problem presented in this study are reported below:

- PC: Intel Core i7-6700 CPU @ 3.4 GHz, 16 GB RAM.
- Operating system: 64-bits Windows 10 Education.
- Programming language: Python 3.5.3 [56]
- Optimisation packages: Pyomo 5.6.1 [54, 57], DEAP 1.3.0 [53]
- Solver: Gurobi 8.1.1 [55]

3. Results

This section presents optimised hybrid solar power plants with TCES for three locations which have different solar resource profiles covering the feasible conditions for solar power plants. The optimisation is performed by the two-stage multi-objective optimisation framework which handles the conflicting objectives, described in the Methodology Section 2. We start by analysing the solar resource of each location before presenting the results of the optimisations.

3.1. Case studies

To analyse and compare the performance of hybrid solar power plants with calcium-looping thermochemical energy storage, and to evaluate the opportunities in the integration of clean technologies to support the transition to a sustainable energy system under different conditions, the model will be evaluated in three locations:

- Seville, Spain, $\approx$ $37.4°N, 6.3°W$
- Tonopah, Nevada, United States, $\approx$ $38°N, 117°W$
- Atacama Desert, Chile, $\approx$ $22°N, 69°W$

The evaluation in each location will result in a distinctive 3-D Pareto surface illustrating the performance expected of an optimised set of different designs in each area. Each point in the Pareto set is a non-dominated solution or potential candidate. Hence, an a-posteriori evaluation of optimised designs for each location should be carried out by the user to select the best hybrid power plant under a trade-off between the objectives or considering other key performance indicators.

3.2. Solar irradiation for the case studies

The typical meteorological year (TMY) is frequently employed to evaluate the feasibility of solar power plants [58]. The TMY is an annual representation of a longer period (e.g. 15 years) of the meteorological conditions in the location, usually with hourly time-steps. There are different open data sources available to obtain the TMY to evaluate renewable power plants [59, 60].

In the present study, the solar irradiation data was collected using three different open data sources: (i) Seville, the "Photovoltaic Geographical information system" (PVGIS project) of the European Commission Joint Research Centre [61]; (ii) Tonopah, System Advisor Model software (SAM-NREL) [44]; (iii) the Atacama Desert, Chilean Ministry of Energy and University of Chile solar resource data centre [62].

To estimate the potential and to compare the solar resource in the three locations, Figure 3 highlights the direct

normal irradiation (DNI) and the global tilted irradiation (GTI) in each area. The DNI is the solar irradiation cap-

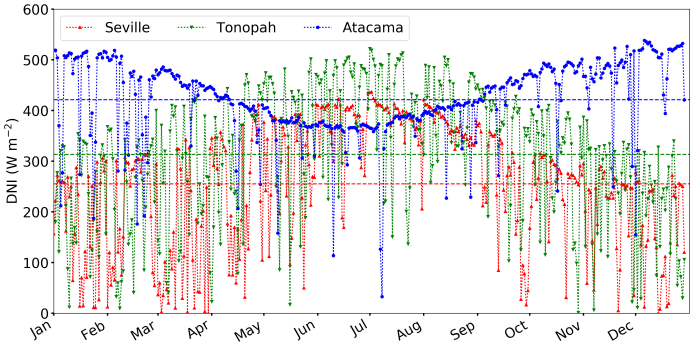

(a) Direct normal irradiation, daily average and annual average

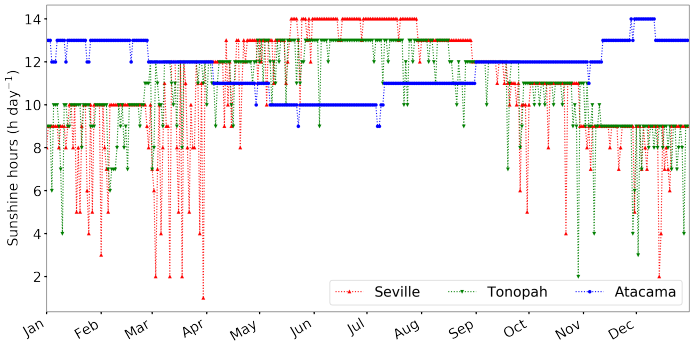

(b) Sunshine hours (hours with $DNI > 0$)

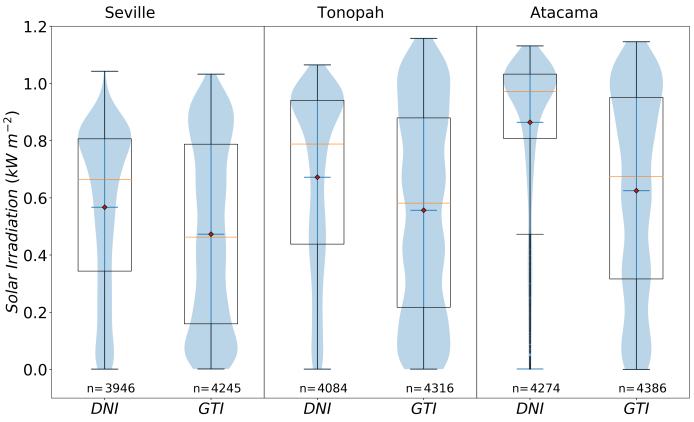

(c) Box and violin plots for DNI and GTI for each location

Figure 3: Solar irradiation of the typical meteorological year for Sevile, Tonopah, and Atacama Desert

tured by the heliostats of the CSP that track the sun. The GTI is the irradiation converted into electricity by the PV plant in which each PV module is non-tracking. Table 2 shows the accumulated annual DNI and GTI considering the typical meteorological year.

Figure 3a presents the DNI daily and annual averages, revealing the difference between each location. Moreover, it can be noted that the variability in the daily DNI of the Atacama Desert is lower than for the other two locations. To support this statement, the standard deviation (σ) of the daily average calculated for Seville, Tonopah, and the Atacama Desert is 120, 130 and 78 W·m^{-2}, respectively. This variability should affect the dispatchability of a CSP plant with TCES if a fixed commitment is required throughout the year.

Table 2: Total direct normal irradiation and global tilted irradiation for the typical meteorological year by location

Location	DNI kWh·m^{-2}·year^{-1}	GTI kWh·m^{-2}·year^{-1}
Seville	2,238	2,006
Tonopah	2,745	2,403
Atacama	3,693	2,742

The variability also can be illustrated in Figure 3b, that shows the total number of sunshine hours per day with a $DNI > 0$. While the average ($\bar{h}_s$) is similar for the three locations ($\bar{h}_{\text{s,Seville}} = 10.8\ h \cdot day^{-1}$, $\bar{h}_{\text{s,Tonopah}} = 10.8\ h \cdot day^{-1}$, $\bar{h}_{\text{s,Atacama}} = 11.7\ h \cdot day^{-1}$), Figure 3b highlights the stable solar resource of the Atacama Desert, i.e. $\sigma_{h,\text{Atacama}} \approx 1\ h \cdot day^{-1}$. In the case of Seville, the higher standard deviation ($\sigma_{h,\text{Seville}} \approx 3\ h \cdot day^{-1}$) shows that there is significantly more variation in the number of sunshine which is due to larger seasonal variations and more cloudy days in winter. A similar trend can be identified for Tonopah, with $\sigma_{h,\text{Tonopah}} \approx 2\ h \cdot day^{-1}$

All these characteristics for the DNI of each location are highlighted in Figure 3c. This figure shows a box plot and a violin plot for the $DNI > 0$ and $GTI > 0$ for the selected locations. The central box in each set of data represents quartiles Q_1 and Q_3 (percentiles 25^{th} and 75^{th}), and the variability of the data set can be estimated by the height of the central box, i.e. the interquartile range or difference between Q_3 and Q_1. Then, the central orange line of each box represents the median of the population, or second quartile (Q_2, i.e. 50^{th} percentile). Next, the whiskers show the extreme values, and some outliers in the case of the DNI of the Atacama Desert can be seen. Besides, the red point located close to the median represents the mean, and at the bottom can be found the total number of samples greater than 0 (from a total of 8760 hours). In addition, the violin plot represented by the light blue area shows the probability density of the samples. For instance, in the case of the DNI of the Atacama Desert, the violin plot shows that the population is concentrated in the top, corroborating the small variability of the direct normal irradiation in the Atacama Desert. The same analysis can be done for the GTI, in this case, the plots show that the means of the GTI follow the same trend than the means of the DNI ($\overline{GTI}_{\text{Atacama}} > \overline{GTI}_{\text{Tonopah}} > \overline{GTI}_{\text{Seville}}$), and the variability can be estimated by the size of the box, or by the distribution of the sample by analysing the violin plots. It can be seen that the variability of the GTI is larger, because, as contrary to the DNI, the GTI is the irradiation in a fixed plane, and even in locations with high solar irradiation, the irradiation in a fixed plane has a large variability throughout the day.

This detailed analysis gives us an idea of the differ-

ence in the design of a dispatchable hybrid solar power plant with TCES in each location. For instance, it could be inferred that a smaller CSP-TCES system is required in the Atacama Desert to supply the same energy during the year. Hence, lower investment and lower LCOE is expected for optimised power plants with a similar level of dispatchability in the Atacama Desert, then Tonopah, and finally, Seville should be the most expensive. Moreover, as outlined before, the high variability in the irradiation in Seville and Tonopah should have a negative effect on the performance of the hybrid solar power plant.

3.3. Optimised designs

The design optimisation aims to select the optimal sizes of the components to design an affordable and dispatchable power plant. Here, the investment cost and the LCOE are used to evaluate the affordability while the loss of power supply probability (LPSP) is used to measure the dispatchability. The LCOE is a crucial indicator that represents the cost of each electricity unit generated over the lifetime of the power plant considering the total life cycle costs, while the investment cost is essential when defining a limiting initial budget for the feasibility of a project. The LPSP measures the mismatch between the net electricity supply and a defined demand, considering one year of operation, i.e. LPSP is the percentage of not fulfilled demand. The multi-objective design optimisation produces a range of Pareto optimal solutions, representing the trade-off between objectives. Figure 4 illustrates the 3-D non-dominated set of solutions at the end of the process.

In each diagram, the x-axis represents the LPSP, the LCOE is shown in the y-axis, and the third objective, the investment cost, is illustrated using different colours. The objective of the design optimisation is to provide affordable and reliable power, thus it is the goal to be located in the bottom left corner of the diagram with low investment costs. Hence, the diagrams reveal the trade-off between technical (LPSP) and financial (LCOE and Investment) performance.

Figures 4a, 4b, and 4c, illustrate the result of the design optimisation in Seville, Tonopah, and the Atacama Desert, respectively. Besides, these figures are merged in Figure 4d to facilitate the comparison of the techno-economic performances of optimised power plants. The non-dominated solutions illustrated in Figure 4a represent potential designs that are optimised through the two-stage optimisation process focused on the simultaneous minimisation of the LCOE and investment cost while maximising the dispatchability. All points shown in Figure 4a are non-dominated, optimal solutions to the problem which means that for a given solution none of the objective values can be improved without degrading at least one other objective.

First, Figure 4a shows that the optimisation process for Seville leads to an improvement of the dispatchability for optimised designs compared with previous results. This improvement is achieved by optimising the capacities of the different components of the energy storage system, which is difficult to handle by a manual optimisation process. The capacities of these components, which are the variables in the design optimisation stage, influence the non-linear interactions of the solar field of the CSP with the sizes of turbines, compressors, heat exchangers, storage tanks and reactors of the TCES system, and the solar field of the PV. In addition, the maximum power dispatch constraint is essential to avoid the design of oversized power plants. For instance, the optimised plant Sev_b, shown in Figure 4a, compared with a manually selected design reported previously in Bravo, Ortiz, Chacartegui, and Friedrich [37], shows that an improved (and not oversized design) can reach similar LCOE and dispatchability with a lower investment. On the other hand, the optimisation process leads to a large decrease of the LPSP, resulting in fully dispatchable power plants at a similar level of LCOE and investment costs. For example, in the case of Seville, and considering an LCOE value of 185 USD·MWh^{-1}, the optimisation process leads to a reduction of the LPSP from 6% to less than 1%. Hence, through the optimisation process, it is possible to get a set of optimal results that can be analysed by the users according to different requirements, improving the decision-making process compared with a manual iterative procedure. This means that the two-stage optimisation routine is an enhanced tool that can be used to analyse the complex interactions between the different components of the hybrid solar power plant and the solar resource. Hence, the results illustrate that optimised designs can achieve simultaneously low cost and high dispatchability.

Table 3: Economic performance metrics of dispatchable power plants

Location	LCOE USD·MWh^{-1}	Investment MUSD	LPSP %
Seville	188	566	0.02
Tonopah	158.5	504	0.01
Atacama	123.4	377	0.01

Table 3 and Figure 5 summarise the economic performance and cost breakdown of highly dispatchable designs, i.e. $LPSP \to 0$ (points Sev_a, Ton_a, and Ata_a in Figures 4a, 4b, and 4c respectively). As explained previously, all non-dominated solutions (Pareto optimal) represent optimised designs. To compare a highly dispatchable power plant with a more affordable power plant (low LCOE), we choose the two extreme points marked with a or b as subindex (e.g. Sev_a, Sev_b) in Figures 4a, 4b, and 4c. Then, the characteristics of these 6 points (2 points per location and three locations) are illustrated in Figure 6. The first section of the diagram corresponds to the objectives and the second section to the variables. Here, the data is scaled regarding minimum and maximum values of each data set shown. For example, the LCOE of Ton_b can be estimated as: $LCOE_{Ton_b} \approx (188.1 - 120.6) \cdot 0.5 + 120.6 \approx 154$ USD·MWh^{-1} (where 188.1 and 120.6 are the maximum and minimum values of the LCOE, respectively, and

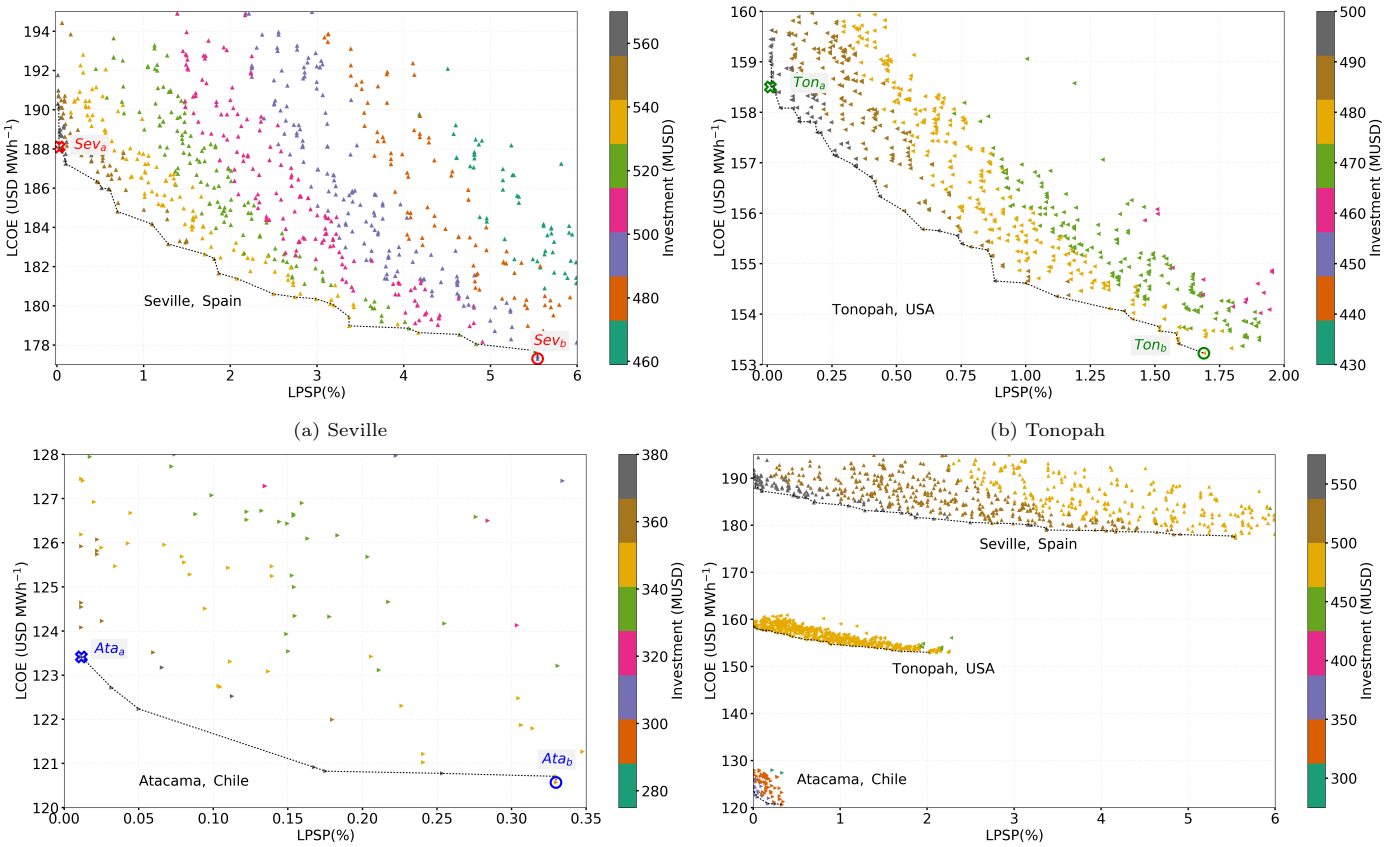

(a) Seville

(b) Tonopah

(c) Atacama Desert

(d) Results of three locations

Figure 4: Results of multi-objective design optimisation. The diagram shows the three dimensional Pareto surface, representing the trade-offs between objectives

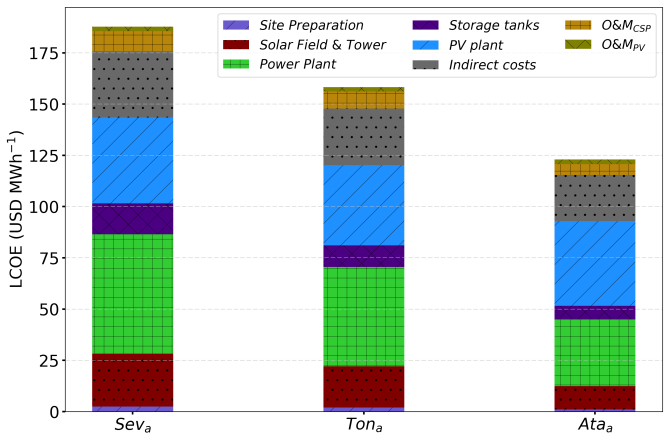

Figure 5: Levelised cost of electricity for dispatchable hybrid power plants

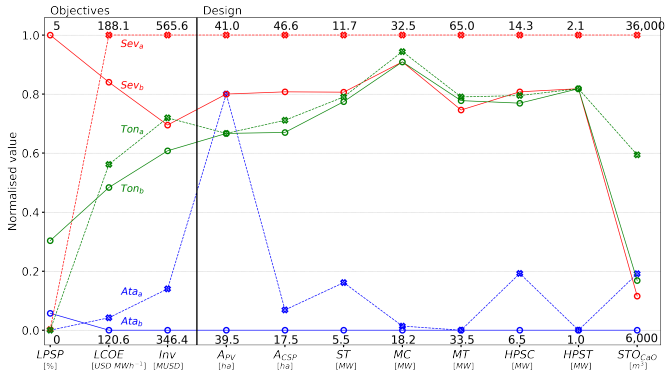

Figure 6: Objectives and configuration of selected optimised designs per location

0.5 is the approximate location of the LCOE for Ton_b, as shown in the figure). The figure shows the large difference in the economic performance of both designs in the Atacama Desert compared with Tonopah and Seville.

Then, it is possible to check the capacity and the range in size between both designs in each location. For instance, the high value in the area of the PV plant for all designs (39.5 ha to 41 ha) demonstrates the benefits of hybridising dispatchable CSP with affordable PV. The ranges in the area of heliostats and the capacities of each turbine and compressor reveal the requirements to design dispatchable power plants. Moreover, the diagram shows a positive cor-

relation between the capacity of each turbine and compressor in the TCES system with the size of the CSP plant. Finally, the three points with the lowest LCOE in each location show a similar capacity of storage. The analysis suggests that there is a relation between the optimised level of storage for these plants and the net capacity of the Brayton cycle. These relations are studied in section 4.2.

3.4. ***Key performance indicators***

In order to compare the operational strategy of different configurations based on measurable results, the following are key indicators for technical and financial performance used in this study:

- E^{net}: total net electric energy dispatched.
- E^{CSP}/E^{net}: total net electricity dispatched by the CSP divided by the total net electricity dispatched by the hybrid power plant. Hence, this value represent the percentage of energy dispatched by the CSP respect to the total.
- $E^{commitment}$: net energy dispatched to fulfil the commitment.
- E^{excess}: the electricity dispatched when the net energy exceeds the commitment (in this model the maximum power that can be dispatched is constrained to five times the commitment).
- $E^{curtailed}$: thermal energy available in the solar field that has to be curtailed.
- $\bar{P}^{net}$: average power dispatched:

$$\bar{P}^{net} = \frac{E^{net}}{8760} \tag{8}$$

- P^{max}: maximum power dispatched by the hybrid power plant over one year of operation.
- P^{max}_{CSP}: maximum power dispatched by the CSP over one year of operation.
- CF_{CSP}: capacity factor referred to the CO_2 Brayton cycle [40].

$$CF_{CSP} = \frac{E^{net}_{Brayton\ cycle}}{P^{max}_{Brayton\ cycle} \cdot 8760} \tag{9}$$

- $\eta_{CSP,CaL}$: efficiency of the CSP considering the energy available and used in the calciner:

[noitemsep]

$$\eta_{CSP,CaL} = \frac{E^{net}_{CSP}}{\sum Q^{Calciner}_{i}} \tag{10}$$

- $\eta_{CSP,DNI}$: overall efficiency considering the solar irradiation in the solar field of the CSP to electricity:

$$\eta^{CSP,DNI} = \frac{E^{net}CSP}{\sum DNI_i \cdot A^{CSP}} \tag{11}$$

- $O\&M$: operational and maintenance costs.

The KPI values are calculated by optimising the annual operation of each design under its respective solar irradiation data and shown in Table 4. These results show that a hybrid solar power plant integrated with CaL has the potential to provide dispatchable power at a cost competitive with current commercial systems. Besides, the values obtained are aligned with those published in a previous paper [39]. In Bravo and Friedrich [39], a large scale ($\approx$ 200 MW) hybrid power plant integrated with thermal energy storage (molten salts) and located in the Atacama Desert was studied. That study concluded that high dispatchability (LPSP $\approx$ 1%) is achieved with an LCOE closer to 122 USD·MWh^{-1}. However, the excellent results obtained with the integration of calcium-looping as TCES process are reached by using natural, widely available and environmentally friendly raw materials (limestone) instead of the use of molten salts or batteries.

4. Analysis and discussion

The results presented in the previous section explore the integration level of each technology under different conditions and provide information supporting the development of renewable and dispatchable power plants. In this section, the results are analysed and used to produce guidelines for the design of hybrid solar power plants with TCES.

4.1. Correlations and ranges

Correlations between the objectives and main variables, i.e. Investment, LPSP, LCOE, A^{CSP}, A^{PV}, and STO (STO^{CaO}) are shown in Figure 7. These correlations help to understand the relations and characteristics of optimised power plants depending on the location. Besides, the ranges of each variable achieved for optimised designs shown in Figure 4 are summarised in Table 5.

4.1.1. All locations

As expected, the high negative correlation between LPSP with A^{CSP}, storage (STO), and investment suggests that CSP and energy storage are crucial to increase dispatchability, and due to the high cost of this technologies, high investment is required. This highlights the importance of energy storage in improving the dispatchability of hybrid power plans. On the other hand, the low correlation between LPSP and A^{PV} means that the solar PV plant does not have an essential effect on the dispatchability.

4.1.2. Seville and Tonopah

First, according to the ranges shown in Table 5, optimised plants in both locations consider a sizeable solar field area for both CSP and PV power plants. Furthermore, the low correlation between the solar PV area (A^{PV}) with the three objectives suggest that the solar PV area

Table 4: Results of the operational optimisation for selected designs per location (as shown in Figures 4a, 4b, and 4c)

KPI	unit	Sev_b	Sev_a	Ton_b	Ton_a	Ata_b	Ata_a
$LCOE$	USD·MWh^{-1}	177.3	188.1	153.2	158.6	120.5	123.5
$LPSP$	%	5.6	0.0	1.7	0.0	0.3	0.0
Invest.	MUSD	498	566	479	504	346	377
E^{net}	GWh·year^{-1}	256	276	288	292	264	279
E^{CSP}/E^{net}	$GWh \cdot year^{-1}/GWh \cdot year^{-1}$	0.49	0.52	0.46	0.47	0.34	0.36
$E^{commitment}$	GWh·year^{-1}	111.7	118.2	116.3	118.2	117.9	118.2
E^{excess}	GWh·year^{-1}	146.1	157.6	171.8	173.6	145.8	160.6
$E^{curtailed}$	$GWh_{th} \cdot year^{-1}$	1.2	2.4	1	2.5	0.5	0.3
$\bar{P}^{net}$	MW	29.4	31.5	32.9	33.3	30.1	31.8
P^{max}_{hybrid}	MW	67.5	67.5	67.5	67.5	67.5	67.5
P^{max}_{CSP}	MW	29.1	33.2	29.7	29.9	17.2	17.1
CF_{CSP}	%	53.5	53.8	55.3	56.8	64.5	73.1
$\eta_{CSP,CaL}$	%	32.5	32.5	32.5	32.5	32.2	32.3
$\eta_{CSP,DNI}$	%	13.8	13.8	13.1	13.0	13.8	13.8
O&M	MUSD·year^{-1}	3.0	3.3	3.0	3.1	2.1	2.1

does not present high variability in optimised plants. In other words, a large solar PV plant is selected in optimised plants, and its capacity is constrained to the maximum power that can be dispatched. On the other hand, the capacity ranges of the components of the CaL system are large (e.g. for Seville the range of the CaO storage tank is from 8,300 to 37,000 m^3), suggesting that the CaL process is the primary variable that influences the results shown in the Pareto diagrams.

Second, the correlations between the investment with the area of the CSP (A^{CSP}) and energy storage, together with the previous statement about LPSP and energy storage, represent the trade-off between dispatchability and affordability in these locations. These numbers suggest that, in Seville and Tonopah, high dispatchability can be reached in power plants with large CSP plants integrated with an extensive TCES system (see Table 5). Moreover, it can be inferred that, in Seville and Tonopah, a large PV is always required to keep a low LCOE, and extra capacity in CSP is required to give dispatchability.

4.1.3. Atacama

As illustrated in Figure 7c, there is a high correlation between the solar PV area with the investment and a high negative relationship between the solar PV area with the LCOE, suggesting that PV improves the affordability in hybrid power plants. These numbers also indicate that a smaller CSP-CaL plant is required to accomplish the commitment (see Table 5), and additional investment in PV results in a considerable reduction in LCOE.

4.2. Design guidelines based on resource and dispatchability

The results shown in Figure 6 were analysed and used to develop guidelines to employ as a starting point for the optimal design of a hybrid solar plant with TCES based on a calcium-looping system. These guidelines are based on the solar irradiation of the three studied locations which cover a range of different solar resources.

Table 5: Ranges of variables for all solutions per location (Figure 4d)

Variable	unit	Seville	Tonopah	Atacama
A^{CSP}	$\cdot 10^4\ m^2$	[33,47]	[35,39]	[17,22]
P^{ST}	MW	[9,14.5]	[8.5,10.5]	[5,8]
P^{MC}	MW	[31,44]	[34,40]	[16,44]
P^{MT}	MW	[55,67]	[58,62]	[30,66]
P^{HPSC}	MW	[17,20]	[16,20]	[7,20]
P^{HPST}	MW	[4,6]	[2.5,5]	[2,8]
STO^{CO_2}	$\cdot 10^3\ m^3$	[1.3,5.7]	[1.5,3.7]	[1,2.3]
STO^{CaO}	$\cdot 10^3\ m^3$	[8.3,37]	[10.8,24]	[6,15]
STO^{Solids}	$\cdot 10^3\ m^3$	[8.4,38]	[11,24.5]	[6.1,15.2]
A^{PV}	$\cdot 10^4\ m^2$	[38,41]	[39,41]	[29,41]

First, as previously stated, a large PV plant will decrease the LCOE in every situation; hence, the optimal design starts by selecting the largest PV area considering the available land and the maximum power that can be dispatched as constraints.

Then, to build equations that relate the capacity of the components of the CSP and CaL system the following variables were combined and manipulated to develop the guidelines: (i) average values that represent the solar resource (number of sunshine hours, direct normal irradiation); (ii) requirements for the operation of the power plant (commitment, dispatchability); (iii) technical performance of the CSP-CaL plant (solar to electricity efficiency); and optimised capacities of the components achieved from the two-stage optimisation routine. As a result of this analysis, equations 13 to 17 were obtained.

First, an approximation of the heliostats field area in

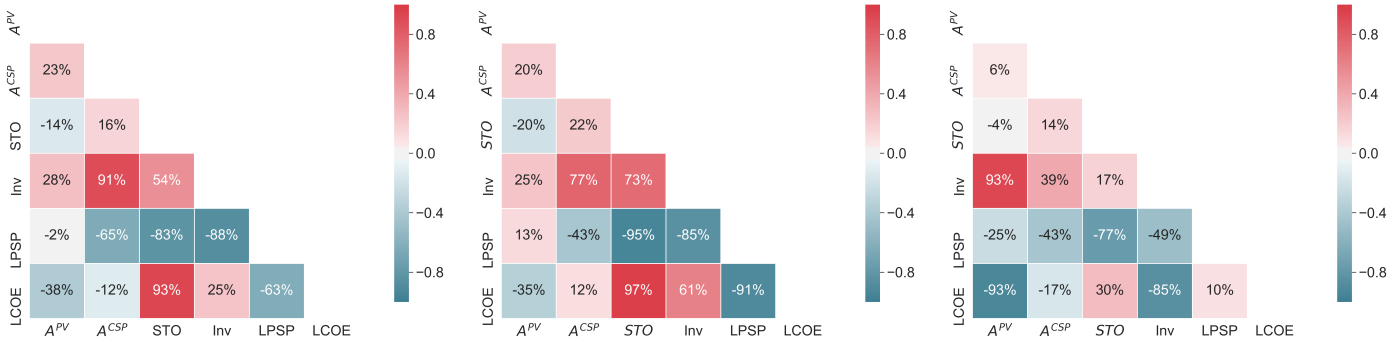

(a) Seville, Spain (b) Tonopah, Nevada, United States (c) Atacama Desert, Chile

Figure 7: Correlations between objectives and design variables in optimised designs

terms of solar resource, technical requirements and performance can be written as:

$$A^{CSP} \approx \frac{P^{commitment} \cdot (24 - \bar{h}_s) \cdot (1 - LPSP)}{\bar{h}_s \cdot DNI_{average} \cdot \eta_{CSP,DNI}} \quad (12)$$

where $\bar{h}_s$ correspond to the average number of sunshine hours, and the LPSP is the flexibility allowed.

Then, as can be seen in Figure 6, the capacities of compressors and turbines are directly related with the heliostat field area. In this context, the capacity of the steam turbine of the Rankine cycle (connected directly to the CSP plant) can be estimated with the thermal power of the CSP plant, through the following equation:

$$P^{ST} \approx A^{CSP} \cdot DNI_{average} \cdot \eta_{CSP,th} \cdot \eta_{SSRC} \quad (13)$$

where $\eta_{CSP,th} \approx 0.36$ and $\eta_{SSRC} \approx 0.268$ [37]. Then, the following relations can be obtained from the optimised designs presented in Figure 6:

$$P^{MC} \approx 3 \cdot P^{ST} \quad (14)$$

$$P^{MT} \approx 1.8 \cdot P^{MC} \quad (15)$$

$$P^{HPSC} \approx 0.4 \cdot P^{MC} \quad (16)$$

$$P^{HPST} \approx 0.15 \cdot P^{HPSC} \quad (17)$$

Finally, the capacity of the energy storage system depends on the relationship between the storage hours and the capacity of the components. Using a specific power generation previously calculated, i.e. $\xi_i \approx 0.053$ MWh·ton$_{CaO}^{-1}$ [37], the capacity of the CaO storage tank (STO^{CaO}, in ton$_{CaO}$) for each location (points Sev_b, Ton_b, Ata_b in Figures 4a, 4b, and 4c respectively) can be estimated by the maximum power dispatched from the Brayton cycle (i.e. $P^{Brayton\ cycle} = P^{MT} - P^{MC}$), according to the following equation:

$$STO^{CaO} \approx \frac{(24 - h_s) \cdot P^{Brayton\ cycle}}{\xi_i} \quad (18)$$

Then, considering a storage density of $\rho_{CaO} \approx 3370$ kg·m^3, and values of porosity and packing density of solids equals to 0.5 and 0.6 respectively [63], it is possible to evaluate the capacity of the storage of CaO in units of volume (m^3). Hence, the capacity of the storage tank of solids and CO_2 can be estimated by:

$$STO^{Solids}(m^3) \approx 1.02 \cdot STO^{CaO}(m^3) \quad (19)$$

$$STO^{CO_2}(m^3) \approx 0.155 \cdot STO^{CaO}(m^3) \quad (20)$$

The application of Equations 12 to 20 generates an initial design of a hybrid solar power plant with TCES which provides a good starting point for further, manual optimisations.

4.3. Sensitivity analysis

A sensitivity analysis was performed for power plants defined as Sev_a, Ton_a, and Ata_a in Figure 4 to determine the influence of key input parameters in the LCOE of dispatchable hybrid power plants. The following parameters, and their original values, were selected for the analysis:

- $\eta^{Receiver} = 0.85$
- $\zeta^{Reactors} = 1$
- $r = 7\%$

where $\zeta^{Reactors}$ is a multiplier used to vary the investment cost of the reactors, i.e. calciner and carbonator; $\eta^{Receiver}$ is the efficiency of the receiver in the solar tower, where the calciner is located; and r is the annual interest rate.

A summary of the sensitivity analysis results is shown in Figure 8. First, we note that the effect of a higher receiver efficiency does not produce a large decrease in the LCOE, because this technical parameter influences both, the LPSP and the LCOE, and these power plants are optimised considering the base value ($\eta^{Receiver} = 0.85$). Nevertheless, in the case that the efficiency is 0.94, the solar field could be reduced, keeping a similar LPSP but reducing the LCOE. For example, for a high receiver efficiency ($\eta^{Receiver} = 0.94$) and a 30% decrease in heliostats area in Atacama, the LCOE reduces to 115 USD·MWh^{-1} ($<$ 121 USD·MWh^{-1}), while maintaining the same LPSP. Hence,

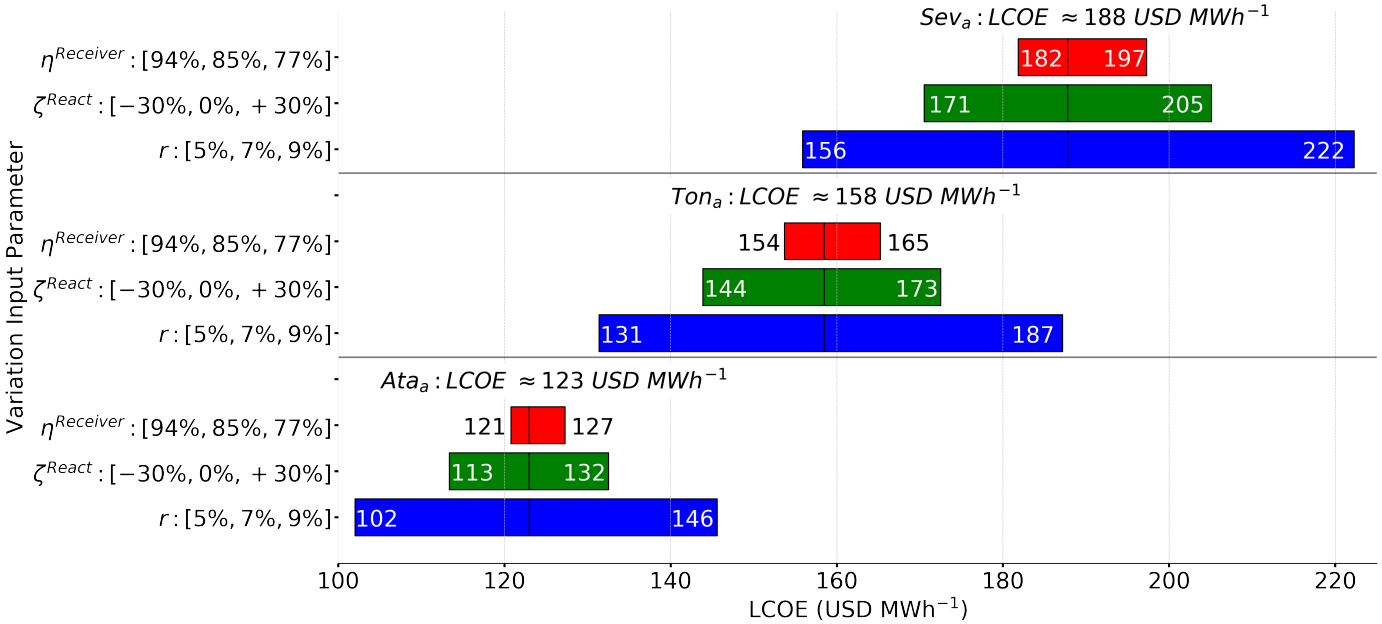

Figure 8: Sensitivity analysis for each location

a further reduction can be achieved by increasing the efficiency of the receiver and modifying the capacity of some components.

We also observe that changes in the investment cost of the reactors and the interest rate have a significant impact on the LCOE. Remarkably, all simulated cases in Atacama (Ata), even in the worst scenarios proposed in the sensitivity analysis, show promising results in terms of LCOE and dispatchability.

4.4. Recommendations for real applications

Our results and analysis highlight the significant advantages to be obtained by optimising the design and operational strategies of solar power plants, according to synergies between solar technologies and energy storage. The results present the benefit of multiple criteria decision making for the design of sustainable, affordable, and dispatchable energy systems, and the importance of handling the trade-offs between conflicting objectives. The guidelines presented can be used in real applications as a first approximation for the economic and optimal design of dispatchable hybrid solar power plants with thermochemical energy storage, based on the solar resource and expected dispatchability. Additionally, the model can be applied to other locations under different input parameters and demand profiles. For example, the cost competitiveness of the power plant would be increased if the power commitment is higher in summer and lower in winter, which would be the case for locations with high cooling demand in summer. In contrast, places like the Atacama Desert whose demand is driven by the intensive mining industry need an almost constant supply of electricity throughout the year. Finally, the model can easily be extended to evaluate different technologies in the hybrid power plant with energy storage.

5. Conclusions

Hybrid solar power plants integrated with thermochemical energy storage are promising candidates to provide dispatchable and affordable clean energy but require sophisticated design tools to achieve this. In this study, we developed a two-stage multi-objective optimisation framework to optimise the design and operation of a hybrid solar power plant (concentrating solar power - photovoltaics) integrated with calcium-looping as thermochemical energy storage system. The optimisation results were used to develop general design guidelines for hybrid solar power plants with thermochemical energy storage systems.

This framework provides key information in the decision-making process for the design of reliable and affordable power plants, going beyond the often used manual design process. Besides, the one-year hourly operational optimisation stage, which takes the seasonal variations in solar resource into account, provides a more suitable design compared to studies which use only a short time horizon or typical periods. The optimisation provides key performance indicators such as affordability, dispatchability, average power supplied, capacity factor, and efficiencies, to compare the performance of different designs and different locations.

The optimisation framework was applied to three locations with different levels of solar irradiation, i.e. Seville, Spain; Tonopah, Nevada, United States; and the Atacama Desert, Chile, to illustrate the opportunities in the integration of clean technologies under different conditions. The

design and techno-economic performance of the optimised plants for each location are clearly defined by the average values and variability of the solar irradiation. Of the three locations, the Atacama Desert has the highest potential, achieving a levelised cost of electricity of 123 USD·MWh^{-1} for a highly dispatchable power plant. This shows the impact of the stability and level of solar irradiation on the design of dispatchable power plants. It also highlights the significant potential of hybrid solar power plants with efficient energy storage systems to provide cost-competitive, dispatchable and clean energy.

The results show that the integration of calcium-looping as thermochemical energy storage system increases the dispatchability of concentrating solar plants with capacity factors as high as 73%, and that the hybridisation with PV plants is essential to achieve competitive energy costs. The results emphasise the potential of the integration of different technologies in the design of affordable and dispatchable renewable power plants to support the transition to a sustainable energy system. While it is clearly shown that multi-objective optimisation is required to achieve an optimal design, this contribution provides general information to understand the interactions and synergies between different technologies, and the opportunities in the development of solar power plants to support the transition to a sustainable energy system.

The optimal designs for the three locations were used to develop guidelines for the optimal design of affordable and dispatchable hybrid solar power plants with calcium-looping as thermochemical energy storage for any location. The guidelines provide an affordable hybrid solar power plant with thermochemical energy storage design based on the solar resource and the required level of dispatchability. While it is only an approximation to the most optimal design, it is an ideal starting point for manual design optimisation in a process simulator such as Ansys. The optimisation framework can provide valuable information for the integration of different technologies to support affordable and sustainable energy systems. Thus, the applied mathematical tools and technologies exposed in this study can support the design of affordable and dispatchable hybrid solar power plants which are required for the transition to a low carbon energy system.

Conflicts of interest

There are no conflicts to declare.

Acknowledgements

Ruben Bravo is supported by a PhD Scholarship from Becas Chile, National Commission for Scientific and Technological Research (CONICYT-Chile), Folio 72160177, 2015. The present research was supported by the Energy Technology Partnership (ETP), International Exchange Grants for Postgraduate and Early Career Researcher Exchanges (PECRE) 2018. Part of this project was developed within the Horizon 2020 Project Socratces, Grant Agreement 727348. Part of this work has been supported by the Spanish Government Agency Ministerio de Economia y Competitividad (MINECO- FEDER funds) under contract CTQ2017-83602-C2 (-1-R and -2-R).

The authors thank Tatiana Bravo for her help with the graphical abstract.

Author Contributions

Conceptualization, R.B., C.O., R.C., and D.F., Methodology, R.B. and D.F., Software, R.B., Validation, C.O., and R.C., Formal Analysis, R.B., and D.F., Data Curation, R.B., C.O., Writing - Original Draft, R.B., Writing – Review & Editing, C.O., R.C., and D.F., Visualization, R.B., Supervision, R.C., and D.F., Project Administration, R.C., and D.F., Funding Acquisition, R.B., C.O., R.C., and D.F.

References

[1] IEA. *World Energy Outlook 2019*. Paris: IEA, 2019. URL: https://www.iea.org/reports/world-energy-outlook-2019.

[2] P. Denholm, J. Jorgenson, M. Miller, E. Zhou, and C. Wang. *Methods for Analyzing the Economic Value of Concentrating Solar Power with Thermal Energy Storage Methods for Analyzing the Economic Value of Concentrating Solar Power with Thermal Energy Storage*. Tech. rep. July. National Renewable Energy Laboratory, 2015.

[3] M. S. Ziegler, J. M. Mueller, G. D. Pereira, J. Song, M. Ferrara, Y. M. Chiang, et al. "Storage Requirements and Costs of Shaping Renewable Energy Toward Grid Decarbonization". In: *Joule* 3.9 (2019), pp. 2134–2153. ISSN: 25424351. DOI: 10.1016/j.joule.2019.06.012.

[4] P. G. V. Sampaio and M. O. A. González. "Photovoltaic solar energy: Conceptual framework". In: *Renewable and Sustainable Energy Reviews* 74 (2017), pp. 590–601. ISSN: 18790690. DOI: 10.1016/j.rser.2017.02.081.

[5] R. Fernández, C. Ortiz, R. Chacartegui, J. M. Valverde, and J. A. Becerra. "Dispatchability of solar photovoltaics from thermochemical energy storage". In: *Energy Conversion and Management* 191 (2019), pp. 237–246. ISSN: 01968904. DOI: 10.1016/j.enconman.2019.03.074.

[6] H. Lund, P. A. Østergaard, D. Connolly, I. Ridjan, B. V. Mathiesen, F. Hvelplund, et al. "Energy storage and smart energy systems". In: *International Journal of Sustainable Energy Planning and Management* 11 (2016), pp. 3–14. ISSN: 22462929. DOI: 10.5278/ijsepm.2016.11.2.

[7] R. Bravo and D. Friedrich. "Integration of energy storage with hybrid solar power plants". In: *Energy Procedia* 151 (2018), pp. 182–186. ISSN: 18766102. DOI: 10.1016/j.egypro.2018.09.045.

[8] A. Zurita, C. Mata-Torres, C. Valenzuela, C. Felbol, J. M. Cardemil, A. M. Guzmán, et al. "Techno-economic evaluation of a hybrid CSP + PV plant integrated with thermal energy storage and a large-scale battery energy storage system for base generation". In: *Solar Energy* 173 (2018), pp. 1262–1277. ISSN: 0038092X. DOI: 10.1016/j.solener.2018.08.061.

[9] M. Liu, N. H. Steven Tay, S. Bell, M. Belusko, R. Jacob, G. Will, et al. "Review on concentrating solar power plants and new developments in high temperature thermal energy storage technologies". In: *Renewable and Sustainable Energy Reviews* 53 (2016), pp. 1411–1432. ISSN: 18790690. DOI: 10.1016/j.rser.2015.09.026.

[10] S. A. Maximov, G. P. Harrison, and D. Friedrich. "Long term impact of grid level energy storage on renewable energy penetration and emissions in the chilean electric system". In: *Energies* 12.6 (2019), p. 1070. ISSN: 19961073. DOI: 10.3390/en12061070.

[11] G. Mohan, M. B. Venkataraman, and J. Coventry. "Sensible energy storage options for concentrating solar power plants operating above 600 °C". In: *Renewable and Sustainable Energy Reviews* 107 (2019), pp. 319–337. ISSN: 18790690. DOI: 10.1016/j.rser.2019.01.062.

[12] A. G. Fernández, J. Gomez-Vidal, E. Oró, A. Kruizenga, A. Solé, and L. F. Cabeza. *Mainstreaming commercial CSP systems: A technology review*. 2019. DOI: 10.1016/j.renene.2019.03.049.

[13] C. Prieto and L. F. Cabeza. "Thermal energy storage (TES) with phase change materials (PCM) in solar power plants (CSP). Concept and plant performance". In: *Applied Energy* 254 (2019). ISSN: 03062619. DOI: 10.1016/j.apenergy.2019.113646.

[14] V. Kashyap, S. Sakunkaewkasem, P. Jafari, M. Nazari, B. Eslami, S. Nazifi, et al. "Full Spectrum Solar Thermal Energy Harvesting and Storage by a Molecular and Phase-Change Hybrid Material". In: *Joule* 3.12 (2019), pp. 3100–3111. ISSN: 25424351. DOI: 10.1016/j.joule.2019.11.001.

[15] C. Ortiz, M. C. Romano, J. M. Valverde, M. Binotti, and R. Chacartegui. "Process integration of Calcium-Looping thermochemical energy storage system in concentrating solar power plants". In: *Energy* 155 (2018), pp. 535–551. ISSN: 03605442. DOI: 10.1016/j.energy.2018.04.180.

[16] D. Kearney, B. Kelly, U. Herrmann, R. Cable, J. Pacheco, R. Mahoney, et al. "Engineering aspects of a molten salt heat transfer fluid in a trough solar field". In: *Energy* 29.5-6 (2004), pp. 861–870. ISSN: 03605442. DOI: 10.1016/S0360-5442(03)00191-9.

[17] K. Vignarooban, X. Xu, A. Arvay, K. Hsu, and A. M. Kannan. "Heat transfer fluids for concentrating solar power systems - A review". In: *Applied Energy* 146 (2015), pp. 383–396. ISSN: 03062619. DOI: 10.1016/j.apenergy.2015.01.125.

[18] J. M. Valverde, M. Barea-López, A. Perejón, P. E. Sánchez-Jiménez, and L. A. Pérez-Maqueda. "Effect of Thermal Pretreatment and Nanosilica Addition on Limestone Performance at Calcium-Looping Conditions for Thermochemical Energy Storage of Concentrated Solar Power". In: *Energy and Fuels* 31.4 (2017), pp. 4226–4236. ISSN: 15205029. DOI: 10.1021/acs.energyfuels.6b03364. URL: https://pubs.acs.org/sharingguidelines.

[19] P. Pardo, A. Deydier, Z. Anxionnaz-Minvielle, S. Rougé, M. Cabassud, and P. Cognet. "A review on high temperature thermochemical heat energy storage". In: *Renewable and Sustainable Energy Reviews* 32 (2014), pp. 591–610. ISSN: 13640321. DOI: 10.1016/j.rser.2013.12.014.

[20] B. Müller, W Arlt, and P Wasserscheid. "A new concept for the global distribution of solar energy: Energy carrying compounds". In: *Energy Environ. Sci.* 4.10 (2011), pp. 4322–4331. ISSN: 17545692. DOI: 10.1039/c1ee01595h.

[21] C. Knoll, D. Müller, W. Artner, J. M. Welch, E. Eitenberger, G. Friedbacher, et al. "Magnesium oxide from natural magnesite samples as thermochemical energy storage material". In: *Energy Procedia*. Vol. 158. Elsevier Ltd, 2019, pp. 4861–4869. DOI: 10.1016/j.egypro.2019.01.707.

[22] R. Chacartegui, A. Alovisio, C. Ortiz, J. M. Valverde, V. Verda, and J. A. Becerra. "Thermochemical energy storage of concentrated solar power by integration of the calcium looping process and a CO 2 power cycle". In: *Applied Energy* 173 (2016), pp. 589–605. ISSN: 03062619. DOI: 10.1016/j.apenergy.2016.04.053.

[23] C. Ortiz, J. Valverde, R. Chacartegui, L. Perez-Maqueda, and P. Giménez. "The Calcium-Looping (CaCO3/CaO) process for thermochemical energy storage in Concentrating Solar Power plants". In: *Renewable and Sustainable Energy Reviews* 113 (2019), p. 109252. ISSN: 13640321. DOI: 10.1016/j.rser.2019.109252.

[24] Y. A. Criado, B Arias, and J. C. Abanades. "Calcium looping CO2 capture system for back-up power plants". In: *Energy Environ. Sci.* 10.9 (2017), pp. 1994–2004. ISSN: 17545706. DOI: 10.1039/c7ee01505d.

[25] M. Bui, C. S. Adjiman, A. Bardow, E. J. Anthony, A. Boston, S. Brown, et al. "Carbon capture and storage (CCS): The way forward". In: *Energy Environ. Sci.* 11.5 (2018), pp. 1062–1176. ISSN: 17545706. DOI: 10.1039/c7ee02342a.

[26] A. Gil, M. Medrano, I. Martorell, A. Lázaro, P. Dolado, B. Zalba, et al. "State of the art on high temperature thermal energy storage for power generation. Part 1-Concepts, materials and modellization". In: *Renewable and Sustainable Energy Reviews* 14.1 (2010), pp. 31–55. ISSN: 13640321. DOI: 10.1016/j.rser.2009.07.035.

[27] J. Obermeier, K. G. Sakellariou, N. I. Tsongidis, D. Baciu, G. Charalambopoulou, T. Steriotis, et al. "Material development and assessment of an energy storage concept based on the CaO-looping process". In: *Solar Energy* 150 (2017), pp. 298–309. ISSN: 0038092X. DOI: 10.1016/j.solener.2017.04.058.

[28] P. E. Sánchez Jiménez, A. Perejón, M. Benítez Guerrero, J. M. Valverde, C. Ortiz, and L. A. Pérez Maqueda. "High-performance and low-cost macroporous calcium oxide based materials for thermochemical energy storage in concentrated solar power plants". In: *Applied Energy* (2019), pp. 543–552. ISSN: 03062619. DOI: 10.1016/j.apenergy.2018.10.131.

[29] C. Ortiz, R. Chacartegui, J. M. Valverde, A. Alovisio, and J. A. Becerra. "Power cycles integration in concentrated solar power plants with energy storage based on calcium looping". In: *Energy Conversion and Management* 149 (2017), pp. 815–829. ISSN: 01968904. DOI: 10.1016/j.enconman.2017.03.029.

[30] M. Petrollese and D. Cocco. "Optimal design of a hybrid CSP-PV plant for achieving the full dispatchability of solar energy power plants". In: *Solar Energy* 137 (2016), pp. 477–489. ISSN: 0038092X. DOI: 10.1016/j.solener.2016.08.027.

[31] D. Salas, E. Tapachès, N. Mazet, and D. Aussel. "Economical optimization of thermochemical storage in concentrated solar power plants via pre-scenarios". In: *Energy Conversion and Management* 174 (2018), pp. 932–954. ISSN: 01968904. DOI: 10.1016/j.enconman.2018.08.079.

[32] A. Alovisio, R. Chacartegui, C. Ortiz, J. M. Valverde, and V. Verda. "Optimizing the CSP-Calcium Looping integration for Thermochemical Energy Storage". In: *Energy Conversion and Management* 136 (2017), pp. 85–98. ISSN: 01968904. DOI: 10.1016/j.enconman.2016.12.093.

[33] R. Renaldi and D. Friedrich. "Multiple time grids in operational optimisation of energy systems with short- and long-term thermal energy storage". In: *Energy* 133 (2017), pp. 784–795. ISSN: 03605442. DOI: 10.1016/j.energy.2017.05.120.

[34] W. J. Platzer. "Combined solar thermal and photovoltaic power plants - An approach to 24h solar electricity?" In: *AIP Conference Proceedings*. Vol. 1734. 2016, p. 130020. ISBN: 9780735413863. DOI: 10.1063/1.4949173. URL: https://doi.org/10.1063/1.4949173https://doi.org/10.1063/1.4984480https://doi.org/10.1063/1.4949230.

[35] A. R. Starke, J. M. Cardemil, R. Escobar, and S. Colle. "Multi-objective optimization of hybrid CSP+PV system using genetic algorithm". In: *Energy* 147 (2018), pp. 490–503. ISSN: 03605442. DOI: 10.1016/j.energy.2017.12.116.

[36] A. Green, C. Diep, R. Dunn, and J. Dent. "High Capacity Factor CSP-PV Hybrid Systems". In: *Energy Procedia*. Vol. 69. 2015, pp. 2049–2059. DOI: 10.1016/j.egypro.2015.03.218.

[37] R. Bravo, C. Ortiz, R. Chacartegui, and D. Friedrich. "Hybrid solar power plant with thermochemical energy storage: a multi-objective operational optimisation". In: *Energy Conversion and Management* 205 (2019), p. 112421. ISSN: 01968904. DOI: 10.1016/j.enconman.2019.112421.

[38] S. A. Kalogirou. "Optimization of solar systems using artificial neural-networks and genetic algorithms". In: *Applied Energy* 77.4 (2004), pp. 383–405. ISSN: 03062619. DOI: 10.1016/S0306-2619(03)00153-3.

[39] R. Bravo and D. Friedrich. "Two-stage optimisation of hybrid solar power plants". In: *Solar Energy* 164 (2018), pp. 187–199. ISSN: 0038092X. DOI: 10.1016/j.solener.2018.01.078.

[40] C. Ortiz, M. Binotti, M. C. Romano, J. M. Valverde, and R. Chacartegui. "Off-design model of concentrating solar power plant with thermochemical energy storage based on calcium-looping". In: *AIP Conference Proceedings*. Vol. 2126. AIP Publishing LLC, 2019, p. 210006. DOI: 10.1063/1.5117755.

[41] IEA. "Technology Roadmap: Solar Thermal Electricity". In: *International Energy Agency, Organisation for Economic Co-operation and Development* (2014). DOI: 10.1007/SpringerReference_7300.

[42] NREL. *Concentrating Solar Power Projects*. 2017. URL: https://www.nrel.gov/csp/solarpaces/ (visited on 06/12/2017).

[43] D. P. Hanak, E. J. Anthony, and V. Manovic. "A review of developments in pilot-plant testing and modelling of calcium looping process for CO2 capture from power generation systems". In: *Energy Environ. Sci.* 8.8 (2015), pp. 2199–2249. ISSN: 17545706. DOI: 10.1039/c5ee01228g. URL: www.rsc.org/ees.

[44] NREL. *System Advisor Model (SAM)*. 2018. URL: https://sam.nrel.gov/.

[45] Cerro Dominador. *Cerro Dominador*. 2020. URL: https://cerrodominador.com/en/proyectos-en/ (visited on 04/27/2020).

[46] J. Cherowbrier. • *Euro to U.S. dollar exchange rate 1999-2018 — Statista*. 2019. URL: https://www.statista.com (visited on 08/14/2019).

[47] S. Michalski, D. P. Hanak, and V. Manovic. "Techno-economic feasibility assessment of calcium looping combustion using commercial technology appraisal tools". In: *Journal of Cleaner Production* 219 (2019), pp. 540–551. ISSN: 09596526. DOI: 10.1016/j.jclepro.2019.02.049.

[48] M. D. Carlson, B. M. Middleton, and C. K. Ho. "Techno-economic comparison of solar-driven SCO2 brayton cycles using component cost models baselined with vendor data and estimates". In: *ASME 2017 11th International Conference on Energy Sustainability, ES 2017, collocated with the ASME 2017 Power Conference Joint with ICOPE 2017, the ASME 2017 15th International Conference on Fuel Cell Science, Engineering and Technology, and the ASME 201*. 2017. ISBN: 9780791857595. DOI: 10.1115/ES2017-3590.

[49] A. Bayon, R. Bader, M. Jafarian, L. Fedunik-Hofman, Y. Sun, J. Hinkley, et al. "Techno-economic assessment of solid–gas thermochemical energy storage systems for solar thermal power applications". In: *Energy* 149 (2018), pp. 473–484. ISSN: 03605442. DOI: 10.1016/j.energy.2017.11.084.

[50] M. Jonemann. *Advanced Thermal Storage System with Novel Molten Salt: December 8, 2011 - April 30, 2013*. Tech. rep. National Renewable Energy Laboratory, 2013. DOI: 10.2172/1080117.

[51] W. Short, D. J. Packey, and T. Holt. *A manual for the economic evaluation of energy efficiency and renewable energy technologies*. Tech. rep. March. National Renewable Energy Laboratory, 1995, pp. 73–81. DOI: NREL/TP-462-5173.

[52] IEA, NEA, and OECD. "Projected Costs of Generating Electricity 2015". In: *International Energy Agency, Nuclear Energy Agency, Organisationf for Economic Co-operation and Development* (2015). ISSN: 16602110. DOI: 10.1787/cost_electricity-2015-en.

[53] F.-A. Fortin, U. Marc-André Gardner, M. Parizeau, and C. Gagné. "DEAP: Evolutionary Algorithms Made Easy". In: *Journal of Machine Learning Research* 13 (2012), pp. 1–5.

[54] W. E. Hart, C. D. Laird, J.-P. Watson, D. L. Woodruff, G. A. Hackebeil, B. L. Nicholson, et al. *Pyomo — Optimization Modeling in Python*. Vol. 67. Springer Optimization and Its Applications. Cham: Springer International Publishing, 2017. ISBN: 978-3-319-58819-3. DOI: 10.1007/978-3-319-58821-6.

[55] L. Gurobi Optimization. *Gurobi Optimizer Reference Manual*. 2019. URL: http://www.gurobi.com.

[56] Python Software Foundation. *Python 3.5.3*. 2017. URL: https://www.python.org/.

[57] W. E. Hart, J. P. Watson, and D. L. Woodruff. "Pyomo: Modeling and solving mathematical programs in Python". In: *Mathematical Programming Computation* 3.3 (2011), pp. 219–260. ISSN: 18672949. DOI: 10.1007/s12532-011-0026-8.

[58] M Sengupta, A Habte, S Kurtz, A Dobos, S Wilbert, E Lorenz, et al. *Best Practices Handbook for the Collection and Use of Solar Resource Data for Solar Energy Applications*. Tech. rep. National Renewable Energy Laboratory, 2015.

[59] Renewables.ninja. *Renewables.ninja*. 2019. URL: https://www.renewables.ninja/ (visited on 01/04/2020).

[60] The World Bank. *Source: Global Solar Atlas 2.0, Solar resource data: Solargis*. Solargis, 2019, pp. 1–6. URL: https://solargis.com/.

[61] J. R. C. European Commission. *JRC Photovoltaic Geographical Information System (PVGIS) - European Commission*. 2017. URL: https://re.jrc.ec.europa.eu.

[62] Ministerio de Energia and Universidad de Chile. *Explorador Solar*. 2016. URL: http://www.minenergia.cl/exploradorsolar/ (visited on 01/11/2020).

[63] J. M. Valverde, P. E. Sanchez-Jimenez, and L. A. Perez-Maqueda. "Limestone Calcination Nearby Equilibrium: Kinetics, CaO Crystal Structure, Sintering and Reactivity". In: *The Journal of Physical Chemistry* (2015). DOI: 10.1021/jp508745u.